

RESEARCH ARTICLE

Speed Up of B2SOLPS5.0 2D Multi-Fluid Code for Tokamak Edge Plasma Simulation

AH Bekheit*

Plasma & Nuclear Fusion Department, Nuclear Research Centre, Atomic Energy Authority, Cairo, Egypt.

*Corresponding author: AH Bekheit, Plasma & Nuclear Fusion Department, Nuclear Research Centre, Atomic Energy Authority, Cairo, Egypt, Tel: + 00201110033615, E-mail: amrhasheim@yahoo.com

Citation: AH Bekheit (2021) Speed Up of B2SOLPS5.0 2D Multi-Fluid Code for Tokamak Edge Plasma Simulation. J Innovations Energy Sci 1: 104

Abstract

Account of drifts and current terms leads to decreases the accessible time step for integration of time dependent equations of B2SOLPS5.0.2D multi-fluid code for tokamak edge plasma simulation. Running the code to solve a large number of fluid transport equations with neutrals and for, various ion species result in the calculation time unacceptably long. In the present article the main method resulting in the time step limit caused by drifts is discussed, which leads to decrease the convergence time to steady state solutions. Applied of this method decreases the time of convergence to the steady state solution.

Keywords: B2SOLPS5.02D; Speed Up; Time Step

Introduction

The physics of the edge plasma behavior and divertor performance is very important for the operation of tokamaks. Traditionally using the fluid transport codes like B2 SOLPS5.02D [1-4] and others depends on Braginskii fluid equations, for parallel (toroidal) transport, experimentally based description of anomalous transport and Monte-Carle model for neutral transport. The B2SOLPS5.2D (Scrape-Off Layer Plasma Simulation) is one of suite codes combines the multi-fluid 2d plasma code B2 with the Monte-Carlo neutrals code EIRENE. It is used in modeling efforts for several experiments design around the world, including studies for ITER. Therefore, we are using this code to simulate the small size divertor tokamak which exists in our department.

Small Size Divertor Tokamak

The basic item of “small size divertor tokamak (SSDT)” is stainless-steel discharge vessel consisting of two toroidal segments insulated from each other and sealed off by an O-ring. The chamber has rectangular cross-section 25 cm by 20 cm. Six large lateral ports and 12 smaller windows at the top and bottom of the vessel allow a good optical access to the entire plasma cross-section. The 180 toroidal field coils TF are directly glued on the vessel by epoxy resin. This makes dismantling and reconstruction of the tokamak very easy (1 day). The computational region for simulation of small size divertor tokamak is based on SN (Single Null) magnetic divertor and covers the SOL (Scrip Off Layer), small part of core and private regions as shown in Figure 1. In computation region the coordinate which vary in the direction along flux surfaces (x-coordinate or poloidal coordinate) and the coordinate which vary in the direction across flux surfaces (y-coordinate or radial coordinate). The computation mesh is divided into 24×96 units (where $-1 \leq x \leq 96$ or $-0.0104 \leq x \leq 1$, $-1 \leq y \leq 24$ or $-0.04166 \leq y \leq 1$) and the separatrix was at $y = 12$. In B2SOLPS5.2D code

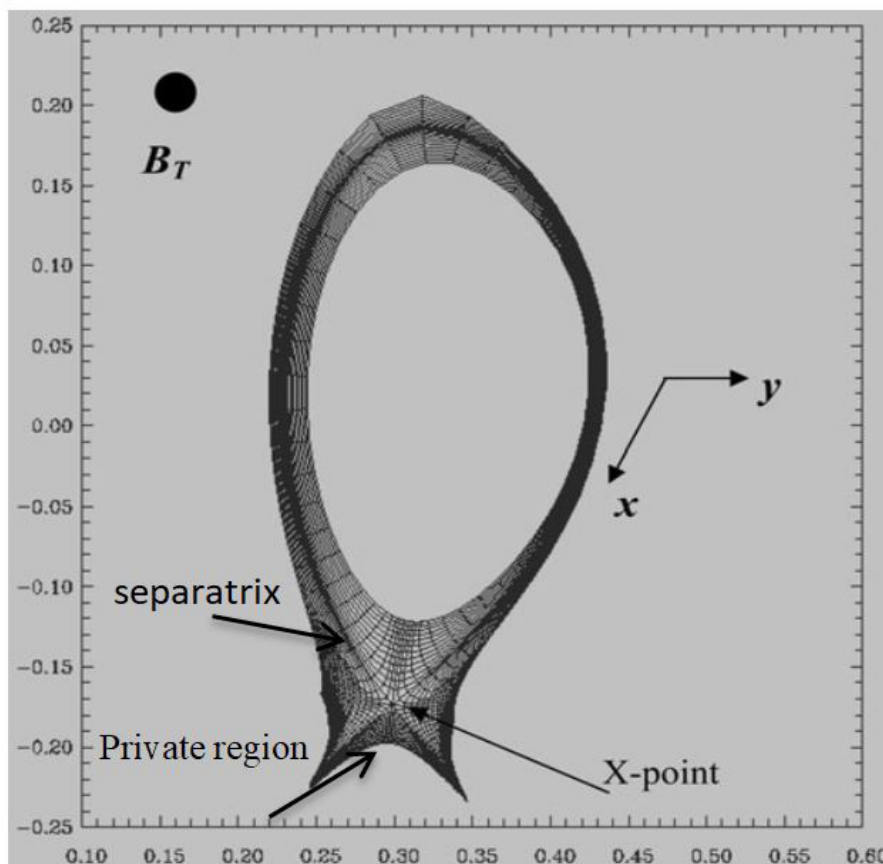


Figure 1: Coordinate system and simulation mesh: x is the poloidal coordinate; y is the radial coordinate orthogonal to the flux surfaces. The directions of magnetic field and Plasma current corresponds to normal operation conditions of SSD tokamak (B drift of ions directed towards the x-point)

the Braginskii transport equation was solved by using field-aligned grids to exactly separate the parallel and perpendicular transport direction. The field-aligned computational grid is created in a preprocessing step. The data structure of B2SOLPS5.2D only supports structured grids, resulting in a global coupling of grid resolution and limiting the possibilities to customize grids for an anticipated solution. During the simulation the grid is fixed, making it impossible for the code to react to changes in the solution. The magnetic field B in a Tokamak is formed by the superposition of an external field generated by magnetic field coils (which determine the general plasma shape) and a field component originating from currents in the plasma (which are driven mainly by induction using a current ramp-up in the central solenoid). The resulting helical magnetic field lines winding around the torus (figure 1) form nested magnetic or flux surfaces (figure 1). In the axially symmetric tokamak case the equilibrium magnetic field configuration balancing magnetic force and plasma pressure is found as the solution of the Grad-Shafranov equation. Equilibrium reconstruction based on the Grad-Shafranov equation is routinely performed for tokamak experiments using interpretive codes and various measurements from diagnostics as input and solution constraints.

In the old versions of B2SOLPS [5-6] self-consistent radial electric fields, drifts, and currents were neglected. These effects were included in the version known as a B2SOLPS5.02D multi-fluid code. The physics of tokamak plasma edge with drifts and currents is treated by this version, however, one to pay a price by a slower convergence of this code. Switch on drifts and current terms in this code dramatically decreases the accessible time step for the solution of time dependent equations of the B2SOLPS5.02D code. Running the code for neutrals and large number of fluid transport equations (Brangnskii equation [1,2] for, various ion species needs boundary conditions (which will introduce in the next section) and makes the computation time unacceptably long. In this article the method of accelerating B2SOLPS5.02D which resulting in time, step limitations and decrease the viscosity coefficient and comparing with non-speeding the B2SOLPS5.02D multi-fluid transport code is analyzed.

The Boundary Conditions

Whether one deals with diamagnetic or $E \times B$ perpendicular drift velocity, special care must be taken to avoid unphysical flows at the plates. The standard boundary condition is to require that the flow be at least sonic at the entrance, which translates into:

$$V_{||} \geq C_s - (b_z / b_x) V_{\perp} \quad (1)$$

Where C_s is the local sound speed and (b_z / b_x) is the inverse of the field line pitch. However, for very small angles as in stellrators the V_{\perp} term may overpower the sound velocity and the boundary condition would require a plasma flow exiting the plate. Therefore, the pitch angle at the plates is limited to be no less than 1 degree, motivated by the engineering limits met when attempting to align the divertor tiles with the magnetic field. The solution procedure of the code was also modified so as ensure that no unphysical flows were being created, and solves the parallel momentum equation using the updated electric potential. Boundary conditions for the current equation at the plate correspond to sheath current – voltage characteristics

$$j_x = en \left[b_x c_s - b_x \frac{1}{\sqrt{2\pi}} \sqrt{\frac{T_e}{m_e}} \exp\left(-\frac{e\phi}{T_e}\right) (1-\gamma) \right] \quad (2)$$

Where γ is the secondary electron emission coefficient. At the inner (core) flux surface the currents are set either to the divergent part of the diamagnetic current or zero. At walls, the same conditions on the normal current components were imposing as for the inner core. The electron and ion heat fluxes to the target plates are:

$$\tilde{q}_{ex} = b_x \frac{n}{\sqrt{2\pi}} \sqrt{\frac{T_e}{m_e}} \exp\left(-\frac{e\phi}{T_e}\right) (1-\gamma) \left(T_e \frac{1+\gamma}{1-\gamma} + e\phi \right) \quad (3)$$

$$\tilde{q}_{ix} = \frac{3}{2} n T_i c_s b_x \quad (4)$$

The simulation by B2SOLPS5.0 2D covering the SOL and a small part of the core as shown in figures (2-4). Therefore, the distance inside the separatrix in all radial profiles in this paper represented this small part of the core which covered by B2SOLPS5.0 2D code.

The Computation Instability Schem

The code B2SOLPS5.2D is depends on the solution of fluid (Branskii) equations for plasma: the heat balance for electron is used to get electron temperature T_e , the heat balance equation for ion used to obtain ion temperature T_i common for all ions species, the current balance equation to obtain electrostatic potential ϕ . The parallel velocity $V_{||}$ and the plasma density n_α for each species “ α ” are found using separate equations of parallel balance, momentum and continuity equation corresponding by the neutral particle are described by either fluid equation or Monte-Carlo EIRENE package. The Branskii fluid equations are linearized and solved by using the Euler method. The main source of iteration result instability is caused by the fact that each equation solved using an implicit technique, but in general the processes of solution of the fluid equation in general is not fully implicit. To obtain the solution of the fluid transport equation the quantities (n , $V_{||}$, T_i , T_e , ϕ) are using quantities calculated previously. The computation instability driven by switch on all drifts and current terms is existed with poloidal redistribution of particles and heat inside the separatrix by $E \times B$ drift associated modification of radial electric field by diamagnetic current. It can be overcome by implementing one of two methods: (1) using artificial factor to slowing down of poloidal distribution of plasma density and temperature. (2) Using a method to modify Branskii fluid transport equations to get faster convergence to be close to the true one, then use it as initial approximation to convergence the true solution. Using these methods leads to decrease the time of convergence to the steady state solution. An additional method to improve the convergence by introducing an artificial increase of time derivatives is also introduced. Therefore, the time step of the iteration processes is limited by the certain shortest characteristic time scales of the processes in which the interplay of main plasma parameters is important. To obtain a very stable algorithm we must solve the fluid equation at a certain time step in a self – consistent manner. Indeed, this numerical method is used in same plasma edge codes, e.g. UEDGE [5]. Unfortunately, the algorithm used increases the solve matrix dimension by a factor 5 for single species plasma, but in the case of plasma with impurities or multi-component plasma the solve matrix is large. For example, pure plasma with Carbon in different charge state $C^{+1 \dots +6}$ the factor is 29. The increase in the computation time for time step together with necessity to reconsider all procedures of the code, makes this way of code improvement not very attractive. Without the introduced methods for small size divertor tokamak parameters, the time step with drifts is of the order of 10^{-6} s. It was found the limiting value of the time step associated with the value of artificial anomalous conductivity $\sigma^{(AN)}$. The artificial current $J^{(AN)} = \sigma^{(AN)} E_y$, $\sigma^{(AN)} = (5-8) \times 10^{-4}$ en (here “e, n” electron charge and plasma density) was first introduced in current balance equation to increase its order to ‘2’ in the y-direction [1]. The anomalous current was retained for convergence purposes. The goal of this paper is to suggest a combination of both approaches give the best result in the framework of the numerical scheme of B2SOLPS5.0.2D code.

Simulation Scheme

The simulations were performed for parameters of small size divertor tokamak (minor radius $a = 0.1$ m, major radius $R = 0.3$ m, $I = 50$ kA, $BT = 1.7$ T). This work focuses on the fluid code B2 in its current Russian version B2SOLPS5.0 2D. A typical plasma solution computed by B2SOLPS5.0 2D covering the SOL and a small part of the core is shown in figure 2-4 [2].

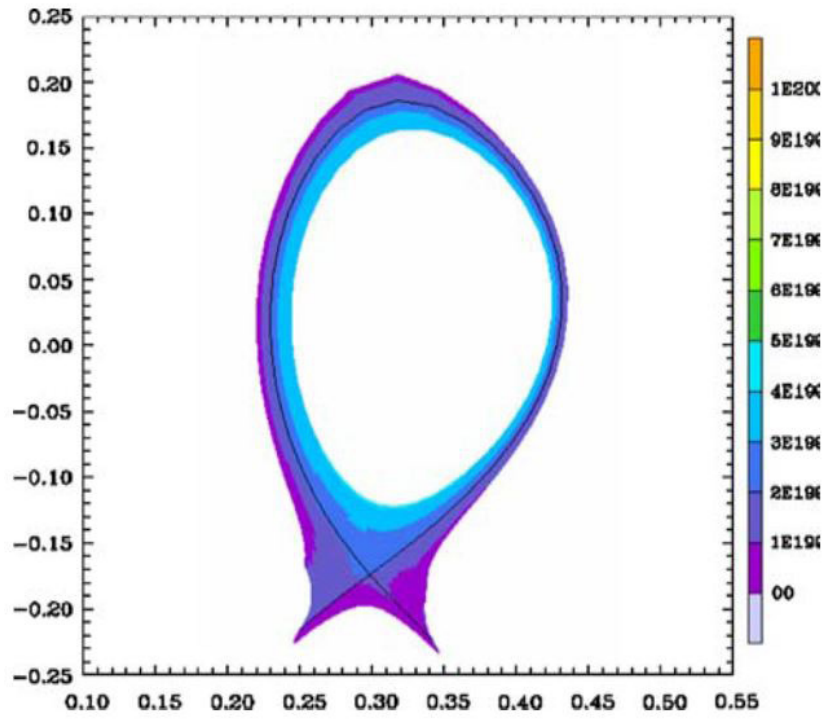


Figure 2: Poloidal distribution of plasma ion density (cm^{-3})

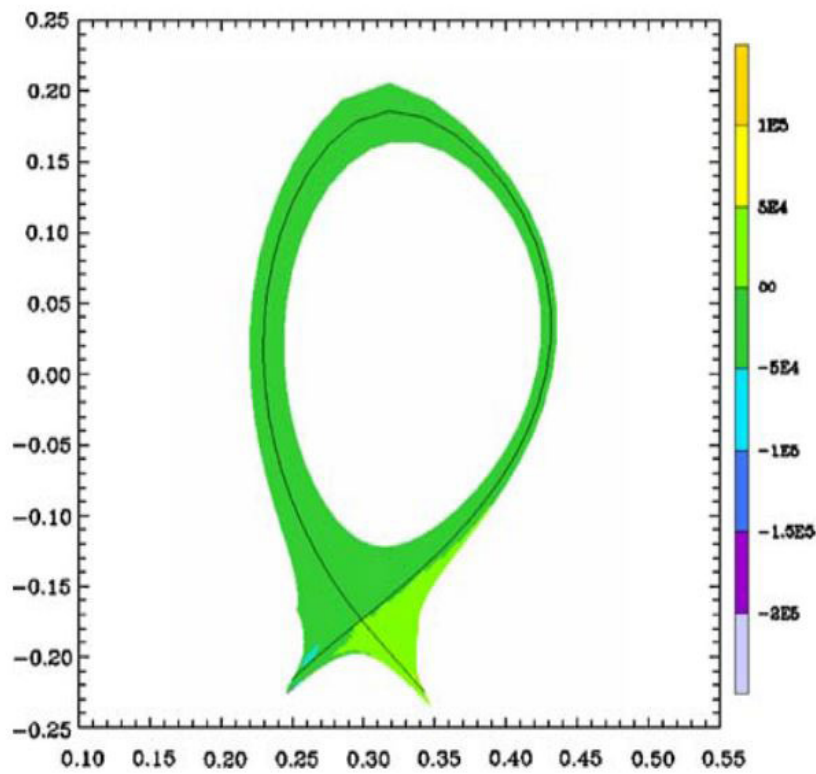


Figure 3: Poloidal distribution of ion parallel velocity

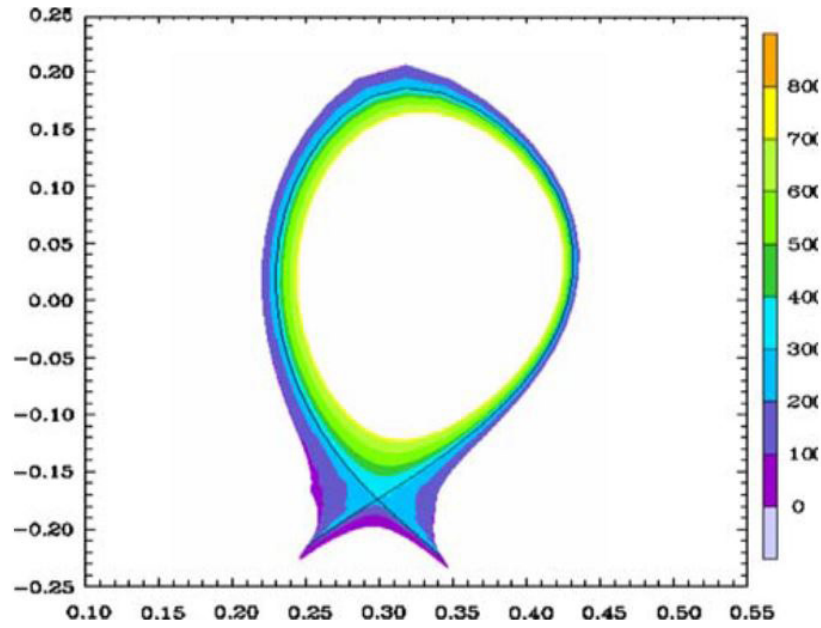


Figure 4: Poloidal distribution of electron temperature (eV)

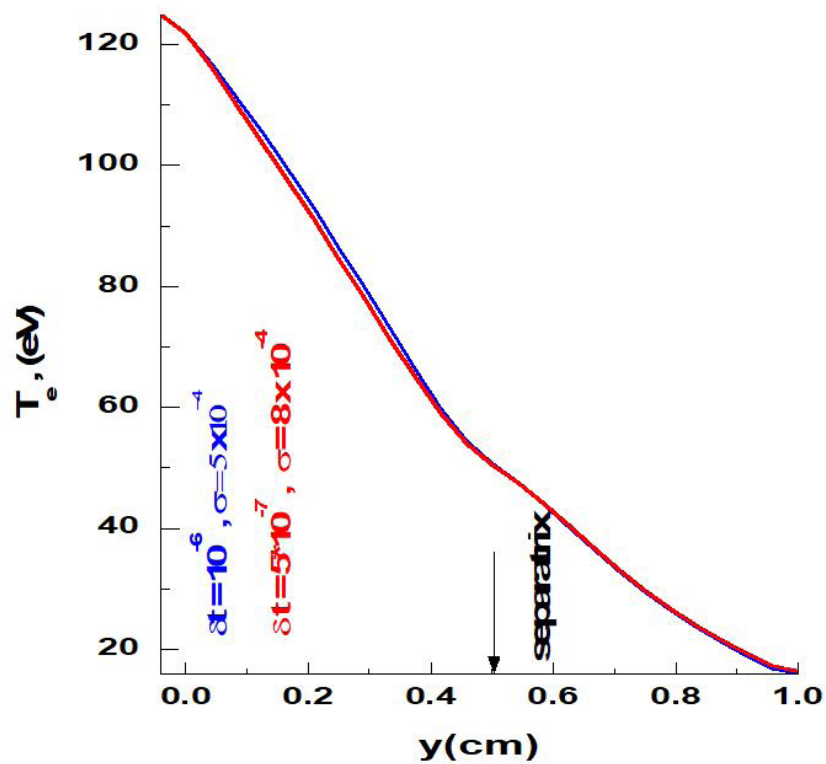


Figure 5: The radial distribution of electron temperature at the first time step $=10^{-6}$ with viscosity coefficient increased two times (blue line) and second time step $=5 \times 10^{-7}$ with decrease viscosity coefficient 70% (red line) from its value

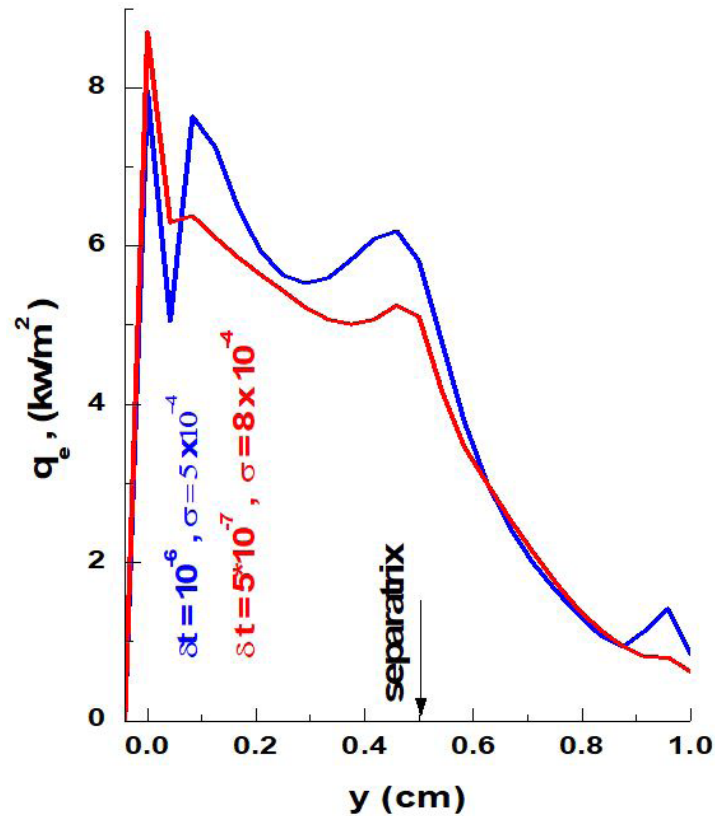


Figure 6: The radial distribution of radial electron heat flux at the first time step $=10^{-6}$ with viscosity coefficient increased two times (blue line) and second time step $=5 \times 10^{-7}$ with decrease viscosity coefficient 70% (red line) from its value

The ideal of the speedup of B2SOLPS5.02D is to obtain first an intermediate solution which is closer to the final true solution running the code with large anomalous radial current. While obtaining a true solution simulations performed with low value of anomalous conductivity σ_{AN} decreasing parallel viscosity coefficient thus permitting small time step. The stage of seeking the solution are, then the following: [1] Increasing time step limit of processes associated with electrostatic potential equation convergence, with increased anomalous conductivity σ_{AN} and increased viscosity coefficient 2 times. [2] Decreased time step to the value limit of processes associated with electrostatic potential equation convergence and decreased both anomalous conductivity σ_{AN} and viscosity coefficient. The plasma parameters of SSD tokamak in the vicinity of the separatrix and in SOL corresponding to the Pfirsch-Schlüter regime, thus justifying the applicability of fluid equations for simulations. The proposed scheme was tested in small size divertor tokamak simulations. The simulation was performed on mesh 24×96 , $T^{(heating)} = 1.05$ keV for plasma with Carbon impurity in different charge states. The preliminary calculations were obtained from (1) time step 10^{-6} s, $\sigma_{AN} = 5 \times 10^{-4}$ with a physical viscosity coefficient increased two times and (2) for time step 5×10^{-7} s, $\sigma_{AN} = 8 \times 10^{-4}$ with decrease viscosity coefficient 70% from its value. The simulation was performed from the solution converged on the two steps with two different times. The comparison of preliminary results of the two steps is shown in figures (5-9). It's seen that the radial profile of electron temperature at the outer midplan did not change. The difference in profiles of electron heat load, radial electric field, ion parallel (toroidal) velocity and plasma density at outer mid plan are changed. The difference in the radial electric field, electron heat load, ion parallel (toroidal) velocity and plasma density are visible in the edge plasma of this tokamak.

The radial space evolution of plasma density at two time stage is shown in Figure (5) shows that redistributed the plasma density at two time stage, at which the radial electric field can be expected to redistribute. The maximum relative change in the plasma density at separatrix is visible on radial scale, about 5%. The radial evolution of plasma density and temperature are shown in figure (5,9). The tracings for speed up B2SOLPS5.02D multi-fluid code with time step 5×10^{-7} s was compared to tracings with time step 10^{-6} s. Again for different time steps leads to the change of the amount of plasma density and temperature in this tokamak is small near separatrix. It can be explained by the small change in the profile of radial electric field redistribution, this change is close to change in the profiles, plasma density and temperature in the vicinity of the separatrix.

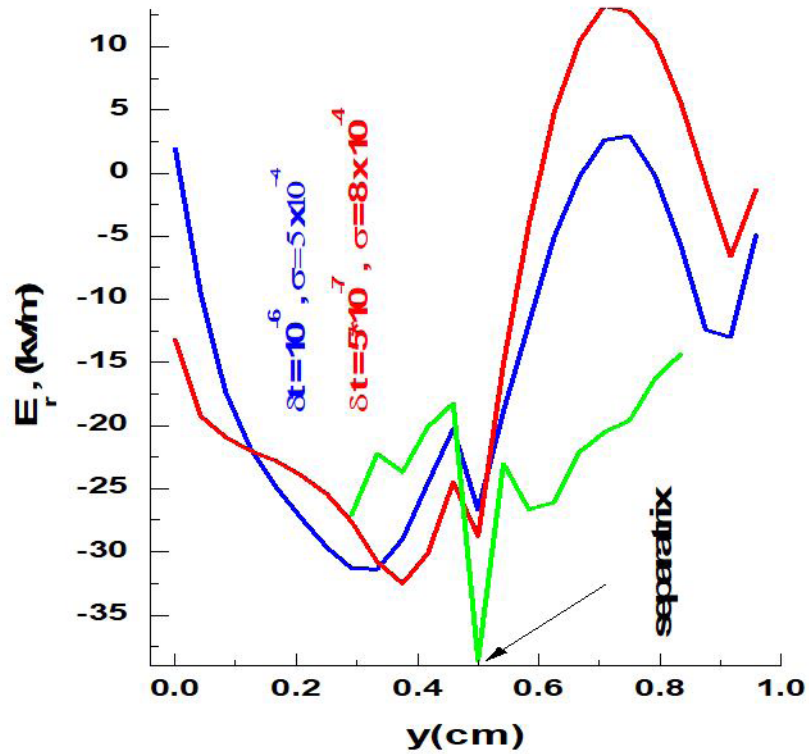


Figure 7: The radial distribution of radial electric field at the first time step $=10^{-6}$ with viscosity coefficient increased two times (blue line), second time step $=5 \times 10^{-7}$ with decrease viscosity coefficient 70% from its value (red line) and neoclassical radial electric field (green line)

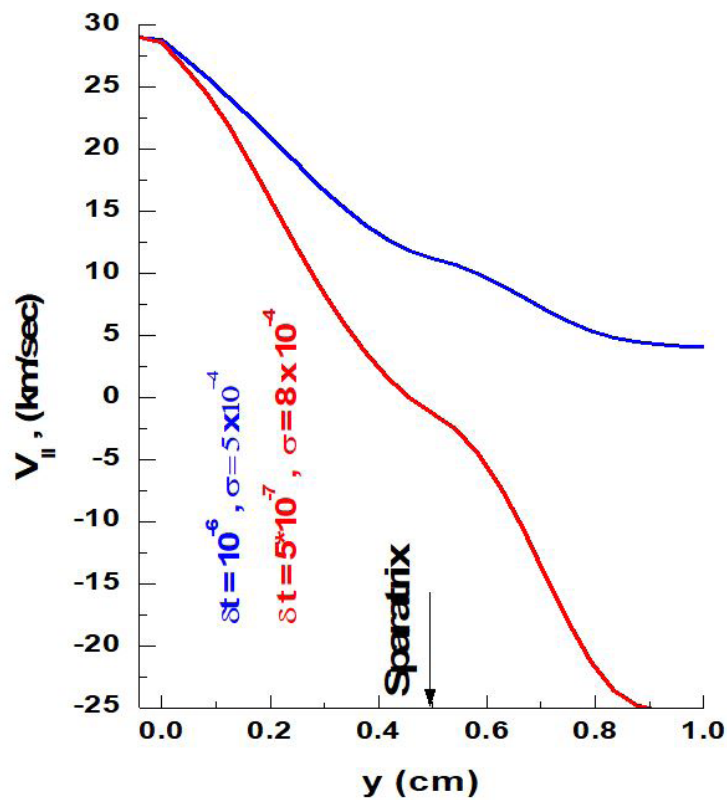


Figure 8: The radial distribution of ion parallel (toroidal) velocity at the first time step $=10^{-6}$ with viscosity coefficient increased two times (blue line) and second time step $=5 \times 10^{-7}$ with decrease viscosity coefficient 70% from its value (red line)

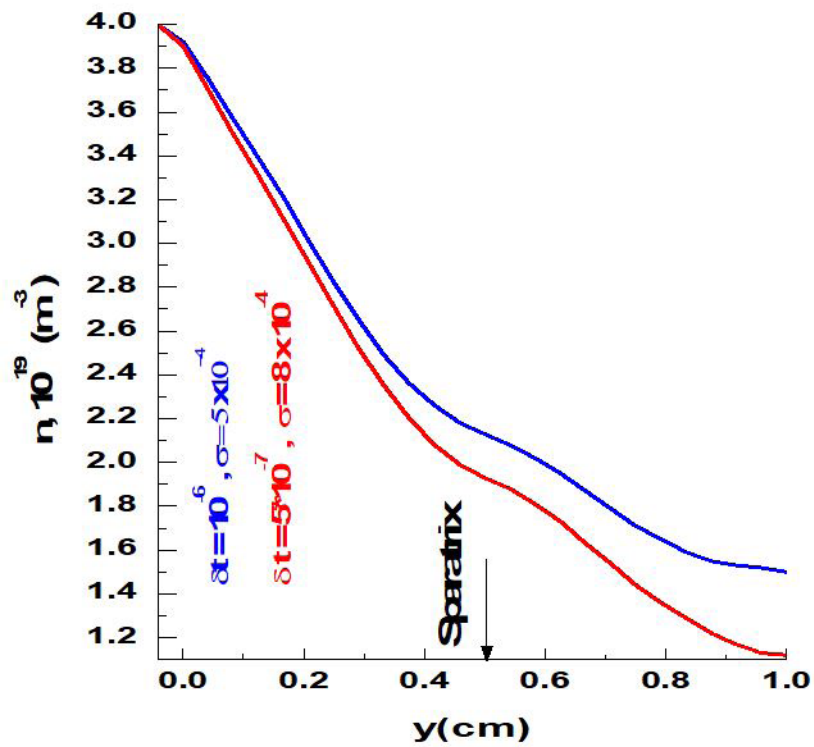


Figure 9: The radial distribution of plasma density at the first time step $=10^{-6}$ with viscosity coefficient increased two times (blue line) and second time step $=5 \times 10^{-7}$ with decrease viscosity coefficient 70% from its value (red line)

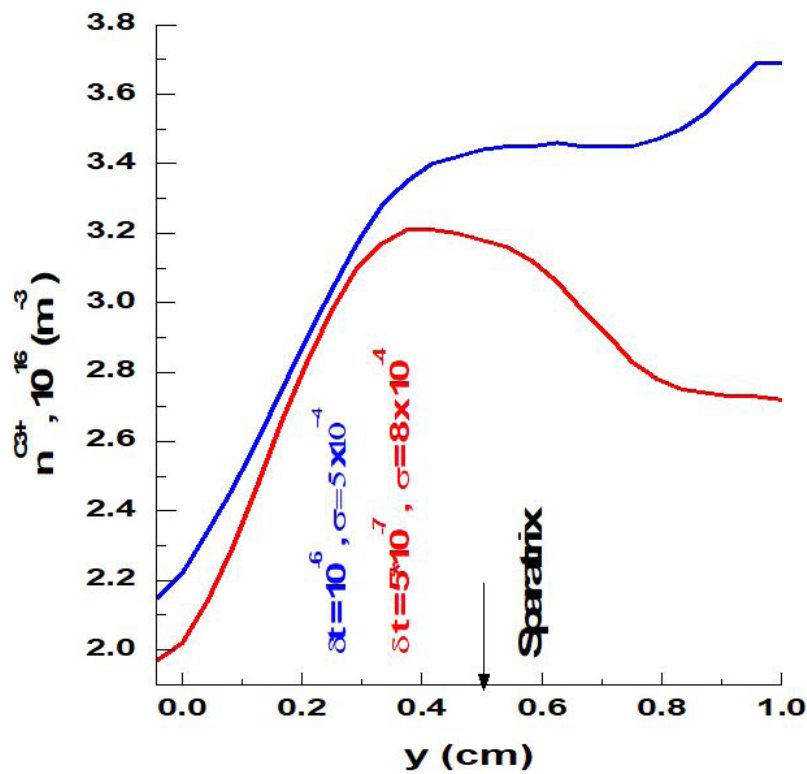


Figure 10: The radial distribution of light Carbon state (e.g. C^{3+}) at the first time step $=10^{-6}$ with viscosity coefficient increased two times (blue line) and second time step $=5 \times 10^{-7}$ with decrease viscosity coefficient 70% from its value (red line)

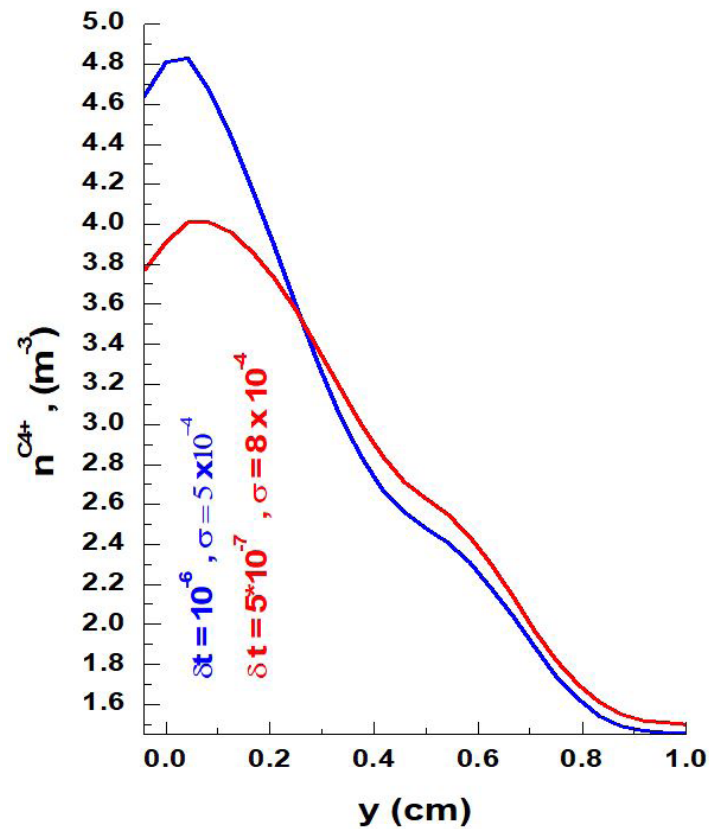


Figure 11: The radial distribution of heavy Carbon state C^{4+} at the first time step $=10^{-6}$ with viscosity coefficient increased two times (blue line) and second time step $=5 \times 10^{-7}$ with decrease viscosity coefficient 70% from its value (red line)

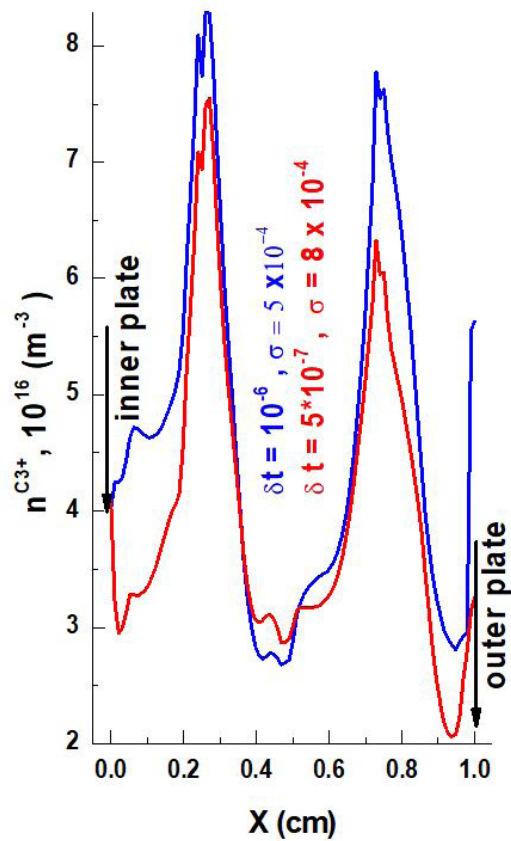


Figure 12: The poloidal distribution of light Carbon impurity (e.g. C^{3+}) at the first time step $=10^{-6}$ with viscosity coefficient increased two times (blue line) and second time step $=5 \times 10^{-7}$ with decrease viscosity coefficient 70% from its value (red line)

So the change radial electric field is close to change of plasma density and temperature (approximately in a neoclassical manner near separatrix, as shown in figure (7)). The density of Carbon impurities in different charge states is shown in figures (10-11) for light (e.g. C^{3+}) and heavy (e.g. C^{4+}) Carbon charge state impurities.

The detailed analysis shows that, the viscosity of plasma change from preliminary time state (at time step 10^{-6} s) to final time stage (at time step 5×10^{-7} s) of the simulation. We conclude that, the plasma viscosity strong influences on the carbon impurities on different charge state distribution inside and outside separatrix more than other parameters. Also, this simulation scheme shows that, the change in ion parallel (toroidal) velocity and radial electric field in the two time stage considering leads to a large difference in the distribution of the carbon impurities in the different charge states in the edge plasma of this tokamak. Therefore, the radial distribution of carbon impurities is very sensitive to details of radial electric field and main ion radial parallel (toroidal) velocity distributions. The analysis of change in $E \times B$ drift velocity due to speeding up B2SOLPS5.02D code gives the value for the change of heavy carbon impurities (e.g. C^{4+}) at the separatrix of about %9.93. The poloidal distribution of light carbon impurities (e.g. C^{3+}) at different time stages are illustrated in figure (12). To speed up the B2SOLPS5.0 2D multi-fluid code leads to large asymmetry in the poloidal distribution of light impurity density with inner plate has a density greater than outer plate. This result indicates that, the friction forces strong influence on the light impurity at inner plate and decrease at outer plate. Therefore, the net friction force at speed up processes directly from the low field side (LFS) to high field side (HFS). Also, this result shows that, at speed up the code the thermal friction forces don't play any role in the distribution of the carbon impurities in the edge plasma of this tokamak which consistent with [6]. The simulation scheme shows that, the radial distribution of the ion of plasma, light and heavy carbon impurities (C^{3+} , C^{4+}) tends to the same value for two times speedup of code B2SOLPS5.02D as shown in figures (13-15). This is can be explained by inside and outside separatrix damps the effect of redistribution of plasma ion light carbon impurity (e.g. C^{3+}) and heavy carbon impurity (e.g. C^{4+}) particles due to the $E \times B$ drifts.

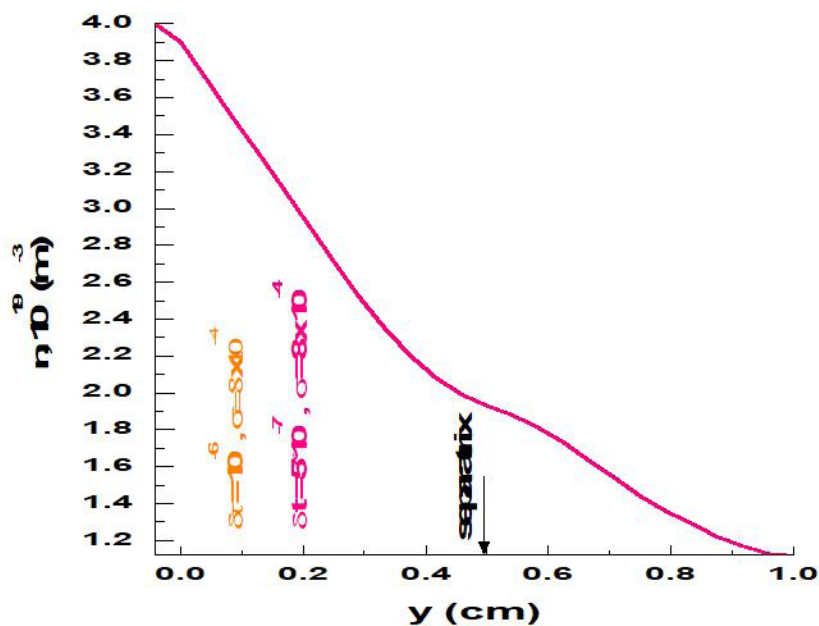


Figure 13: The radial distribution of plasma ion at the first time step $=10^{-6}$ with viscosity coefficient decrease 70% from its value (orange line) and second time step $=5 \times 10^{-7}$ with decrease viscosity coefficient 70% (pink line) from its value

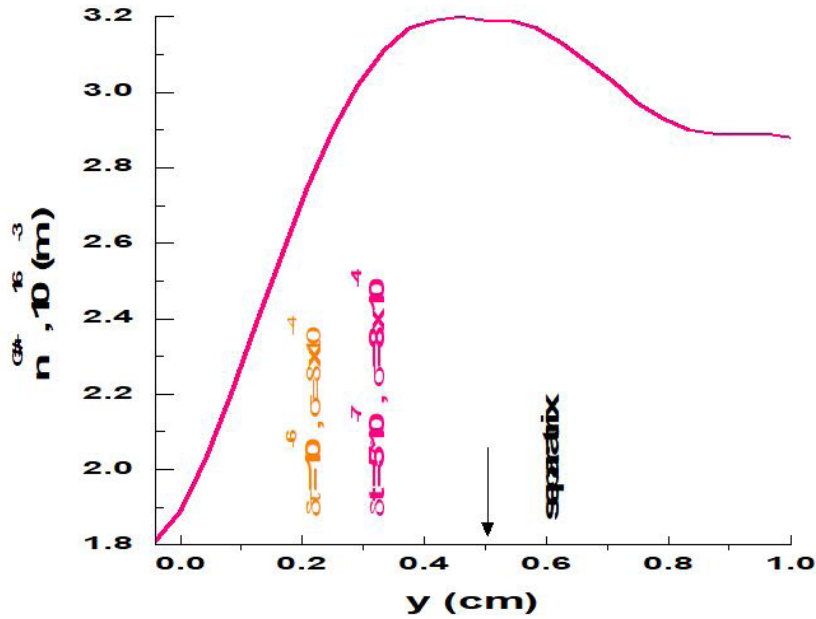


Figure 14: The radial distribution of light Carbon state C^{3+} at the first time step $=10^{-6}$ with viscosity coefficient decrease 70 % (orange line) from its value and second time step $=5 \times 10^{-7}$ with decrease viscosity coefficient 70% (pink line) from its value

The test of converged solution was performed at the next step. The speedup scheme was applied to decrease the viscosity coefficient 70% for the time step 10^{-6} s then after the convergence results the time step was decreased to 5×10^{-7} s with fully viscosity coefficient. The evolution of simulation results is shown in Figures (16-17). shows that, no great change during the speed up turning off. The time step limitation from B2SOLPS5.02D multi-fluid code is approximately 10^{-6} s, therefore further increase of convergence speed is limited by B2SOLPS5.02D multi-fluid code. Since a large time the evolution of the system is approximate the same with or without speed up the increase.

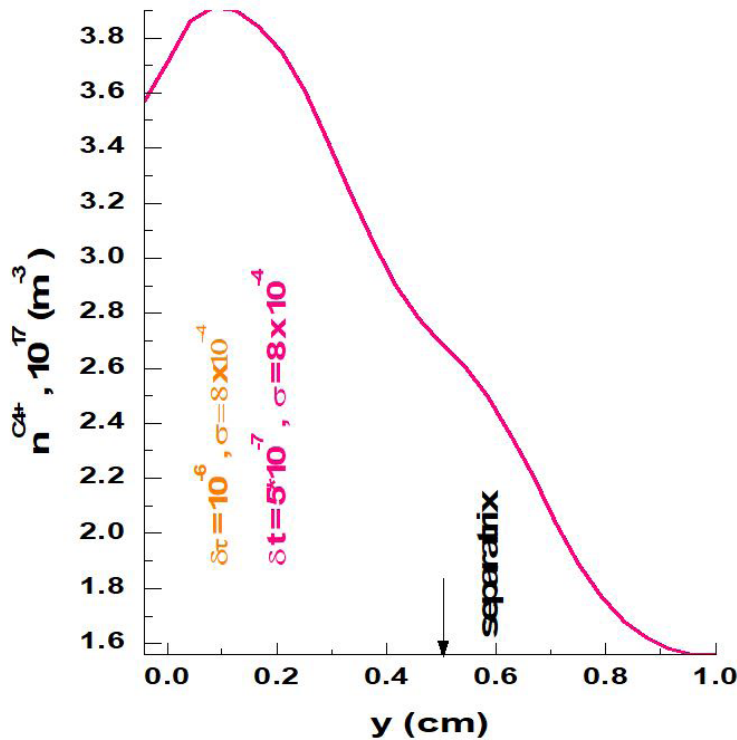


Figure 14: The radial distribution of heavy Carbon state C^{4+} at the first time step $=10^{-6}$ with viscosity coefficient decrease 70 % (orange line) from its value and second time step $=5 \times 10^{-7}$ with decrease viscosity coefficient 70% (pink line) from its value

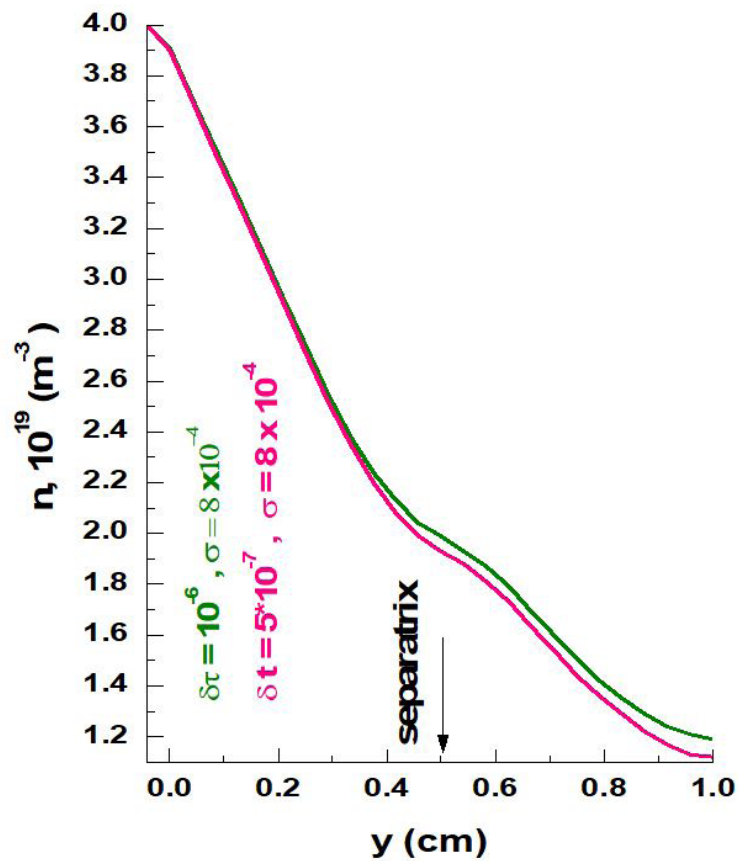


Figure 16: The radial distribution of plasma ion at the first time step = 10^{-6} with viscosity coefficient decrease 70% (olive line) from its value and second time step = 5×10^{-7} with a full viscosity coefficient (pink line) from its value

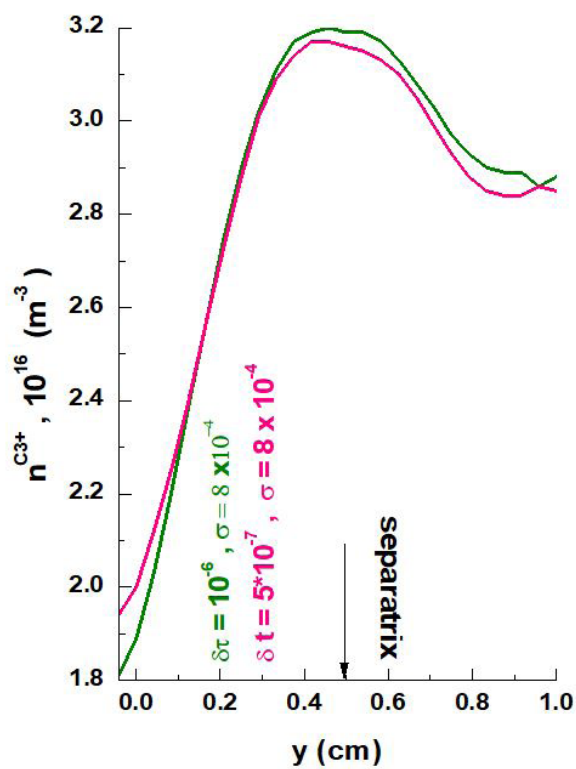


Figure 17: The radial distribution of light Carbon state C^{3+} at the first time step = 10^{-6} with viscosity coefficient decrease 70 % (olive line) from its value and second time step = 5×10^{-7} with a full viscosity coefficient (pink line) from its value

Conclusion

Simulation of edge plasma of small size divertor tokamak with full B2SOLPS5.02D multi-fluid code, including EIRENE neutral and charge particle drift are enabled with acceptable convergence time scales, only with the implementation of improved numerical schemes. The challenging which found of the convergence time step is related to the poloidal redistribution of particles and heat inside the separatrix by drift. It can be solved by artificial reduction of the largest characteristic time scales. The speed up the B2SOLPS5.02D multi-fluid code strong influence on the distribution of radial electric field, electron heat load, ion parallel (toroidal) velocity and plasma density at the two time stages considered. Also the change radial electric field is close to change of plasma density and temperature (approximately in a neoclassical manner vicinity of the separatrix). We notice the detail analysis shows that, the viscosity of plasma change preliminary time stage (at time step 10^{-6} s) to final time stage (at time step 5×10^{-7} s) of simulation influences on the different charges state of carbon impurities more than other parameters. Simulation results show that, the radial distribution of carbon impurities is very sensitive to details of radial electric field and main ion radial parallel (toroidal) velocity distribution in the edge plasma of this tokamak. The analysis of $E \times B$ drift velocity due to speeding up B2SOLPS5.02D multi-fluid code result in a change in the density of high charge state of carbon impurities C^{4+} in the separatrix of about 9.93%. Also the simulation results indicate that, the friction forces strong influence on the light impurity at inner plate and decrease at outer plate. Therefore, the net friction force at speed up processes directly from the low field side (LFS) to high field side (HFS) and thermal friction force don't play any role. The radial distribution of plasma ions, light and heavy impurities (e.g. C^{3+} , C^{4+}) in the edge plasma of this tokamak at two different times speedup of B2SOLPS5.02D code are the same. This explained by redistribution of (e.g. Plasma ion, C^{3+} and C^{4+}) particles damps due to $E \times B$ drifts in the edge plasma of this tokamak. The evolution of simulation results shows that, no great change during speed up turning off. The time step limitation from B2SOLPS5.02D code is approximately 10^{-6} s.

Reference

1. R Schneider, V Rozhansky, V Voskoboynikov (2001) Nucl Fusion 41: 387.
2. AH Bekheit (2008) J Fusion energy 27: 338-45.
3. AH Bekheit (2016) J Fusion energy 35: 769-75.
4. AH Bekheit (2017) J Nuclear Energy Sci Power Generation. Technol 6: 2.
5. Braams B J Contrib (1996) Plasma Phys. 36: 276.
6. Schneider R, Bonnin X, Coster DP, Kastelewicz H, Reiter D, et al. (2006) Contrib. Plasma Phys. 46: 3
7. TD Rognlien, JL Milovich, ME Rensink, GD Porter, HJ Nucl (1992) Mater 8: 347.
8. R Schneider, V Rozhansky, V Voskoboynikov, AH Bekheit etc (2003) J Nucl Mater 313-6, 1141-9.